Roughness Element Geometry Required for Wind Tunnel Simulations of the Atmospheric Wind

I. S. GARTSHORE
Associate Professor.

K. A. DE CROOS
Research Assistant.

Dept. of Mechanical Engineering,
The University of British Columbia,
Vancouver, B. C., Canada

Using a data correlation for the wall stress associated with very rough boundaries and a semi-empirical calculation method, the shape of boundary layers in exact equilibrium with the roughness beneath them is calculated. A wide range of roughness geometries (two- and three-dimensional elements) is included by the use of equivalent surfaces of equal drag per unit area. Results can be summarized in a single figure which relates the shape factor of the boundary layer (its exponent if it has a power law velocity profile) to the height of the roughness elements and their spacing. New data for one turbulent boundary layer developing over a long fetch of uniform roughness is presented. Wall shear stress, measured directly from a drag plate is combined with boundary layer integral properties to show that the shear stress correlation adopted is reasonably accurate and that the boundary layer is close to equilibrium after passing over a streamwise roughness fetch equal to about 350 times the roughness element height. An example is given of the way in which roughness geometry may be chosen from calculated equilibrium results, for one particular boundary layer thickness and a shape useful for simulating strong atmospheric winds in a wind tunnel.

1 Introduction

The neutral atmospheric boundary layer can be simulated in a wind tunnel by creating a thick turbulent boundary layer on one surface of the tunnel (usually the floor) so that measurements can be made in the turbulent region with models of appropriate scale. Upstream of the model, which may include scaled sections of an urban area for example, the thick turbulent boundary layer is developed by combinations of spires, wedges or trips together with roughness elements distributed on the wall. Various techniques have been used (see discussions by Davenport and Isyumov [1],[1] Standen [2], and Counihan [3]) but in each case the wall roughness geometry used was apparently chosen by trial and error and not because it produced a predictable wall shear stress or velocity distribution. This work provides a relation between roughness geometry and velocity profile shape which should allow a more rational choice of the roughness to be made for any desired profile or effective wall shear stress.

The equilibrium of boundary layers used for atmospheric simulations is often mentioned and is usually implied, although the term equilibrium is seldom defined precisely. What is usually meant by equilibrium is that boundary layer characteristics such as velocity profile shape, nondimensional spectra, etc., are not changing significantly in the streamwise direction. A more exact form of equilibrium is defined by the term "self-preservation" used by Townsend [4]. Self preservation describes a turbulent shear flow whose turbulence is in exact dynamic equilibrium so that the mean distributions of the turbulence, nondimensionalized by a single velocity and length scale, do not change at all in the streamwise direction. Such exact equilibrium is strictly possible for rough wall boundary layers in zero pressure gradient only when certain rather artificial conditions are satisfied: either the roughness elements are high compared to their spacing (which must be regular) producing the "d-type" roughness described by Perry, et al. [5] or else the roughness height and spacing must vary directly with streamwise distance so that each remains a constant fraction of the boundary layer height, as described by Rotta [6].

Some analytical results implied by exact self-preservation are presented in Section 4 of this paper.

A restricted region of a boundary layer with zero pressure gradient and constant roughness height and spacing is in approximate equilibrium provided the start of the roughness or any change in roughness is far from the region considered. Mellor

[1] Numbers in brackets designate References at end of paper.

Contributed by the Fluids Engineering Division and presented at the Winter Annual Meeting, New York, N. Y., December 5, 1976 of THE AMERICAN SOCIETY OF MECHANICAL ENGINEERS. Manuscript received at ASME Headquarters August 11, 1976. Paper No. 76-WA/FE-18.

and Gibson [7] have concluded that turbulent zero-pressure-gradient boundary layers on smooth walls closely conform to the requirements for exact equilibrium over limited streamwise lengths, and it seems reasonable to assume that the same is true for rough-wall boundary layers. A discussion of this point is included in Section 6 of this paper.

In order to estimate the roughness which is required to produce certain boundary layer characteristics, even for approximate equilibrium, it is necessary to formulate some relationship for the wall shear stress in terms of other boundary layer properties. The streamwise development of the flow can then be predicted by any one of a variety of well known semi-empirical methods. These two steps are outlined in the next two sections, followed by a presentation of the exact equilibrium results implied by the simple method adopted. Some new experimental evidence on rough wall boundary layers is then presented and the approach to equilibrium is discussed. Finally a procedure is suggested for estimating the roughness required to produce a desired boundary layer shape needed for atmospheric simulation, and an example is given of this procedure.

2 A Wall Stress Relationship for Rough Walls

The flow around individual roughness elements at high Reynolds numbers is not yet predictable in detail from the equations of motion. Previous empirical work has related the wall shear stress to some integral boundary layer thickness, usually the displacement thickness (δ^*), and this empirical approach is followed here.

A rather extensive review of the results obtained using square two-dimensional bar roughness elements has been made by Dvorak [8] who related the bar height (k) and the bar spacing (λ_e) to the effective wall shear stress (τ_0) and displacement thickness δ^*, using the form proposed by Clauser [9], as follows:

$$\frac{U_1}{U_\tau} = \frac{1}{K} \ln \left\{ \frac{U_1 \delta^*}{U_\tau k} \right\} + A - C. \tag{1}$$

where: $\dfrac{U_\tau}{U_1} = \left\{ \dfrac{\tau_0}{\rho U_1^2} \right\}^{1/2}$

with U_1 = free stream velocity

A = constant = 4.8

K = constant = 0.41

and C is a constant depending on λ_e and k as follows:

$$C = -5.95 \left[0.48 \ln \frac{\lambda_e}{k} - 1 \right] \tag{2}$$

This correlation is valid for $(\lambda_e/k) > 5$ and for $(U_\tau k/\nu) > 70$, both satisfied in most atmospheric simulations of high winds.

Few natural rough boundaries can be approximated by a pattern of square bars normal to the flow and it is necessary to generalize these results to three-dimensional roughness elements of various shapes. This is done here by defining an effective spacing between two-dimensional bars which produces surface drag per unit area (or average shear stress) equal to that of the more general roughness pattern.

The drag of a unit width of a single two-dimensional square bar (subscript b) is:

$$D_b = C_{Db} \frac{1}{2} \rho \bar{U}^2 k$$

where k is the height of the bar and $\bar{U}$ the average velocity approaching it. The drag per unit area is then $D'_b = D_b/\lambda_e$ where λ_e is the spacing between the bars in the flow direction.

Similarly, the average drag of a unit area of general three-dimensional elements each of similar shape and each having a drag coefficient C_{DR} based on its frontal area, is

$$D'_R = \frac{C_{DR} \frac{1}{2} \rho \bar{U}^2 A_F}{(\lambda R)_1 (\lambda R)_2}$$

where $(\lambda R)_1$ and $(\lambda R)_2$ are spacings between element centers in the lateral and the longitudinal directions respectively and A_F is one element's frontal area. Equating D'_R to D'_b for equal $\bar{U}$:

$$\frac{C_{Db} k}{\lambda_e} = \frac{C_{DR}}{(\lambda R)_1} \frac{A_F}{(\lambda R)_2}$$

This can be rewritten as:

$$\frac{\lambda_e}{k} = \frac{(C_D)_b}{(C_D)_R} \frac{A_p}{A_F} \tag{3}$$

where $A_p = (\lambda R)_1 (\lambda R)_2$ is the effective plan area associated with each element. The ratio (λ_e/k) is now the equivalent spacing of two-dimensional bars of height k which produces wall stress equal to the general roughness whose height is also k.

The drag co-efficients $(C_D)_b$ and $(C_D)_R$ vary with varying upstream boundary layers, but we assume that the ratio of one to the other will remain constant for identical upstream conditions and identical heights of bar and roughness element. We further assume that the mean characteristics of the turbulent boundary layer, and its turbulent properties as well, are dependent only on the value of the effective wall shear stress, so that two roughness patterns which produce identical local wall stress will produce identical boundary layers. These assumptions remain to be tested in detail but they produce plausible and tentatively useful relationships.

We must now determine the ratio of $(C_D)_b$ to $(C_D)_R$ measured with identical element heights and identical upstream boundary layers. If the upstream boundary layer is considerably smaller than the height k, the drag co-efficient of a surface-mounted square plate normal to the flow is about 1.15, and that of a two-dimensional surface-mounted plate infinitely wide normal to the

Nomenclature

A_F = frontal area of one roughness element
A_p = plan area associated with one roughness element
A = 4.8, constant associated with equation (1)
C = function of roughness geometry, equation (2)
H = δ^*/θ, shape factor for boundary layer
H_1 = shape factor related to H by equation (6)
K = von Karman's constant, taken to be equal to 0.41
k = roughness element height
n = shape factor related to H by equation (13); equal to the exponent of a power law velocity profile if equation (7) is valid
U = mean velocity at height Z
U_1 = free stream velocity (constant)
U_τ = $[\tau_0/\rho]^{1/2}$ shear velocity
x = streamwise distance, measured from start of roughness
Z = distance normal to wall
δ = nominal boundary layer thickness, related to δ^* and n by equation (11)
δ^* = displacement thickness
θ = momentum thickness
λ_e = effective streamwise spacing of two dimensional bars; see also equations (3) and (4)
ρ = density of fluid (constant)
τ_0 = average shear stress on roughened wall

flow is about 1.20. A cube in the same circumstances has a drag co-efficient of about 1.17 and a long square bar normal to the flow, four times as wide as it is high, has a value of 1.2. These results, all taken from the compilation of reference [10], suggest that the ratio $(C_D)_b/(C_D)_R$ is close to unity for some shapes of roughness element. In particular, this approximation appears valid for parallelepiped-shaped elements having one face normal to the flow, depth less than or equal to height and width greater than about 0.4 times the height [see reference [10]]. For other shapes of roughness element, drag coefficients must be estimated or measured for use in equation (3).

Since the rectangular elements described in the previous paragraph imply a drag co-efficient ratio of approximately one, equation (3) for these elements becomes:

$$\frac{\lambda_s}{k} \simeq \frac{A_F}{A_P} \tag{4}$$

Equations (3) or (4) allow the shear stress correlation of Dvorak to be used for a wide variety of two- and three-dimensional roughness shapes.

3 A Calculation Method

Having used integral properties in the shear stress correlation of the previous section, it is now sensible to adopt an integral calculation method to predict the streamwise development of the boundary layer.

As pointed out by Dvorak [8], an integral auxilliary equation which is based on the entrainment of fluid through the outer edge of the turbulent region is preferable to those based on integral properties of shear stress or kinetic energy through the layer. The latter methods may be particularly sensitive to the roughness geometry through the uncertain conditions very close to the individual roughness elements. For this reason, we follow Dvorak in using Head's empirical correlations. Head's method is described by Dvorak and in reference [11]. Applied to zero-pressure-gradient boundary layers, it becomes:

$$\frac{d}{dx}(\theta H_1) = F_1\left[\frac{\delta^*}{\theta}\right] \tag{5}$$

where F_1 is a known empirical function of the ratio (δ^*/θ), θ is the usual momentum thickness and H_1 is a shape factor related empirically to (δ^*/θ) [see equation (6)]. For the range of (δ^*/θ) expected in atmospheric simulations, $F_1(\delta^*/\theta)$ can be represented, following Dvorak, as:

$$F_1\left(\frac{\delta^*}{\theta}\right) = \exp\left[-3.512 - 0.617 \ln (H_1 - 3)\right]$$

$$\text{where:} \quad H_1 = 3.3 + \exp\left[0.4667 - 2.722 \ln (H - 0.6798)\right] \tag{6}$$

$$\text{and} \quad H = \frac{\delta^*}{\theta}$$

It is not necessary to assume a form for the velocity profile to use this method, but if the simple power law is used for other purposes, it can be related to H in the usual way: if

$$\frac{U}{U_1} = \left[\frac{Z}{\delta}\right]^n \tag{7}$$

the exponent n is equal to $(H - 1)/2$.

As in all integral methods, the momentum integral equation:

$$\frac{d\theta}{dx} = \left[\frac{U_\tau}{U_1}\right]^2 \tag{8}$$

is also used. Thus, equation (1) describing the shear stress, and equations (5) and (8) describing the development, can be used to predict the streamwise variation of the three boundary layer properties U_τ, θ and δ^*. Equations (1) and (2), relating (U_τ/U_1) to δ^* for given k and λ_s are shown graphically in Fig. 1. The differential equations (5) and (8) must be solved numerically for particular cases of interest, unless the boundary layer is in exact equilibrium. In this case, the differential equations become arithmetic as shown in the next section.

4 Results for Exact Equilibrium

If the velocity profile shape is not changing at all, i.e. δ^*/θ and H_1 are constant, the equations of the previous section adopt even simpler forms. It is useful to demonstrate this, since zero-pressure-gradient boundary layers developing over a constant roughness geometry may conform approximately to this equilibrium condition.

If (δ^*/θ) = constant, then H_1 = constant from equation (6). Equation (5) then shows that $d\theta/dx$ is a constant, so that the boundary layer grows linearly. Equation (8) shows that U_τ/U_1 = constant in any one such equilibrium case, which is strictly possible from equations (1) and (2) only when λ_s/k and δ^*/k remain constant, as already mentioned. By combining equations (8) and (5) to eliminate θ, we may relate H to U_τ/U_1 as follows:

$$\left[\frac{U_\tau}{U_1}\right]^2 = F_1(H)/H_1 = \text{function of } (H) \tag{9}$$

where F_1 and H_1 are related to H in equation (6). The shape factor H can be related to n which can in turn be interpreted as the exponent of the power law profile if equation (7) is adopted. Notice that n can be regarded as a shape factor even if equation (7) is not an accurate description of the velocity profile however.

The shear stress ratio (U_τ/U_1) occuring in (9) can be replaced by suitable functions of δ^*/k and λ_s/k as shown in Fig. 1 or equations (1) and (2) so that (9) can be written as:

$$n = \frac{H-1}{2} = fn\left[\frac{U_\tau}{U_1}\right] = fn\left[\frac{\delta^*}{k}, \frac{\lambda_s}{k}\right] \tag{10}$$

Since,

$$\frac{\delta^*}{k} = \frac{\delta}{k}\left[\frac{n}{n+1}\right] \tag{11}$$

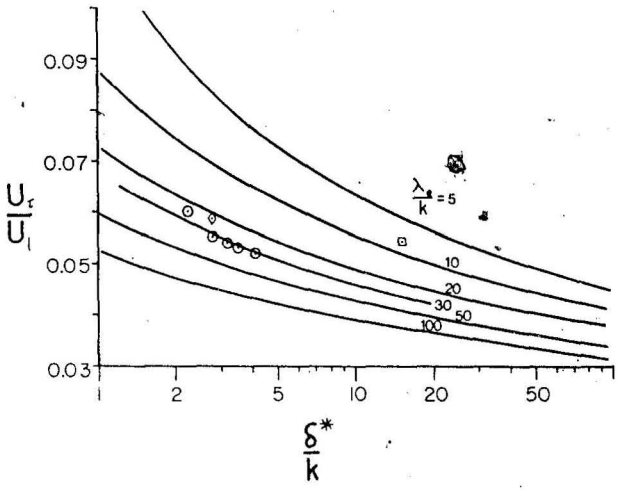

Fig. 1 Wall shear stress expected for various roughness geometries. Dvorak's correlation (8) ———; present data ⊙; O'Laughlin from Wooding, et al. [14], λ_s/k = 64, ◇; Antonia and Luxton, [12], λ_s/k = 4, ⊡.

can be used to define a nominal boundary layer thickness δ, equal to the actual boundary layer thickness if a power profile exists, equation (10) can be written as:

$$n = fn\left[\frac{\delta}{k}, \frac{\lambda_s}{k}\right] \tag{12}$$

as plotted in Fig. 2. Notice that this relationship is valid only for equilibrium situations, since the arithmetic relationship of equation (9) is applicable only for exact equilibrium.

The ratio $[U_1\delta^*/(U_\tau\delta)]$ is related to the defect law, as pointed out by Clauser [9] (see also reference [11]). He found that both rough and smooth wall boundary layers have the same value of $[U_1\delta^*/(U_\tau\delta)]$ in zero-pressure-gradient, implying a truly universal defect law. The present equilibrium calculations do not give a precisely constant value of this parameter over the entire range of λ_s/k and n considered. Calculated values lie between 3.80 and 3.99, compared to Clauser's value of 3.60 for boundary layers developing over constant roughness. These values will be discussed in Section 6.

5 Present Measurements

To compare with the calculated results of Figs. 1 and 2, particularly for three-dimensional roughness elements, measurements were made in a boundary layer developing over a long fetch of uniformly roughened wall.

The U.B.C. wind tunnel used for these experiments is an open-circuit, blower type and has a test section 24.4 m in length, 2.44 m wide, and initially 1.5 m in height. The test section roof is adjusted to maintain ambient room pressure throughout the test section length. Mean velocity measurements were made using a linearized hot wire anemometer.

The floor roughness was created by fastening thin vertical strips of aluminum to the wall at regular intervals. Each strip presented a frontal area of 38.1 mm high and 19 mm wide to the flow. The strips were placed in lines across the tunnel, the strips being 152.4mm apart in each line and the lines being 152.4 mm apart using a staggered pattern.

The resultant value of A_P/A_F for equation (3) is 32 and, using the assumption that the drag coefficients in this equation are equal, the value of λ_s/k obtained from equation (4) is also 32.

A small trip was used at the beginning of the roughness fetch to reduce the importance of any length of smooth surface upstream of the roughened wall and to reduce the importance of the initial roughness elements. (See a discussion of this point by Antonia and Luxton, reference [12]). The trip used was a wedge

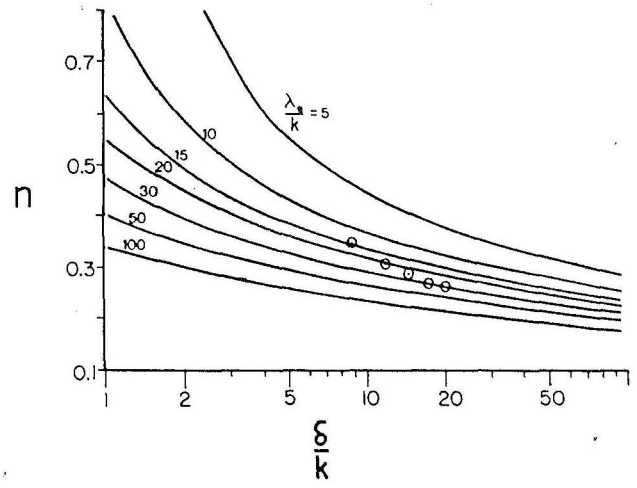

Fig. 2 Effect of roughness geometry on profile shape. Exact equilibrium conditions, _____; present data, ⊙.

38.1 mm thick and with 203 mm chord placed across the entire tunnel so that it created a gradual two-dimensional ramp and then a backward facing step 38.1 mm high.

Wall shear stress was measured directly from a drag plate, a large isolated section of roughened floor fastened to an accurate wind tunnel balance. The drag force on this section could then be measured directly and the average force per unit area deduced. This drag plate was 0.91 m wide and approximately 2 m long, so that reasonably large drag values were obtained. Drag readings were found to be insensitive to the size of the small gap around the drag plate but were sensitive to tunnel pressure gradient. The latter was set as carefully as possible to zero for each test. Drag readings were found to be proportional to the square of the free stream velocity, as expected, indicating that no Reynolds number effects were present. The drag plate measurements and the boundary layer parameters δ, δ^*, θ and n deduced from the measured velocity profiles are discussed here, since they are directly comparable to the correlations of previous sections. Measured values of δ^* and θ and values of n and δ deduced from them are given in Table 1.

Table 1 Measured boundary layer properties

$\frac{x}{k}$	$\frac{\delta^*}{k}$	$\frac{\theta}{k}$	n	$\frac{\delta}{k}$	$\frac{U_1}{U_\tau}$	$\frac{U_1\delta^*}{U_\tau\delta}$
140.8	2.17	1.28	0.348	8.38	16.48	4.27
268.8	2.83	1.75	0.309	11.93	17.97	4.26
332.8	3.25	2.06	0.289	14.44	18.41	3.14
396.8	3.51	2.27	0.273	16.49	18.74	3.99
492.8	4.08	2.67	0.264	19.73	18.98	3.92

NOTES

1) k = 1 1/2 in. (38.1 mm)
2) The boundary layer thicknesses δ^* and θ were obtained by integration from measured velocity profiles; δ and n were then deduced from δ^* and θ.
3) U_τ was found from force measurements on the drag plate.
4) Roughness Reynolds number U_1k/ν, was approximately 3×10^4.

The values of δ^* and θ were obtained by integration directly from the measured velocity profiles. Values of H are equal to the ratio (δ^*/θ) [see equation (6)] and n may be calculated from:

$$n = \frac{H-1}{2} \tag{13}$$

The quantity n is used here simply as a shape factor, related to H through equation (13). In fact, the velocity distributions were not particularly well described by a relationship of the form of equation (7), so that the more laborious but precise approach described above was necessary. The nominal boundary layer thickness δ was then found from equation (11). Values of δ as calculated were close to the values of δ which might have been chosen from the velocity profiles themselves. As is well known, the definition of δ directly from the measure velocity profiles is somewhat arbitrary, and has been avoided through the present procedure.

For experimental convenience, measurements with different lengths of roughness fetch were made, not by moving the drag plate from one place to another, but by adding or subtracting roughness sections upstream of the fixed point of measurement. Thus, the measurements do not relate precisely to a single boundary layer, since upstream of each fetch of roughness (x), there is a variable length of smooth floor equal to the tunnel length minus x. Perhaps for this reason, the measured values of θ were slightly but consistently larger than those obtained by use of the two-dimensional momentum equation [equation (8)] together with measured values of shear stress. A difference of 11 percent was found between the two values of θ at the maximum fetch of

roughness when measured values of θ at the shortest roughness fetch were used as the starting condition for the integration of equation (8).

The experimental uncertainty of the data is estimated as follows: U_τ/U_1, ± 3 percent; δ^*/k, ± 2 percent; θ/k ± 2 percent; n (based on uncertainties in δ^* and θ), ± 4 percent; δ/k (based on uncertainties in δ^* and n), ± 6 percent. Uncertainties in x and k are negligible.

6 Discussion of Experimental Results

The measured values of δ^*/k, θ/k, U_1/U_τ and n are plotted in Figs. 1 and 2.

The calculated curves of Fig. 1 do not assume an equilibrium condition, but merely represent the shear stress correlation of Dvorak [8]. The measured values in this figure agree with the trends of the data and indicate that the effective value of λ_e/k for the present data is about 30, which is close to the value expected from the geometrical arrangement as calculated from equation (4) ($\lambda_e/k = 32$). Thus, we have some confidence in the shear stress correlation of Dvorak and in the present extension of it to three-dimensional roughness elements.

A comparison with the data of two other experiments is made in Fig. 1: that of O'Laughlin, reported by Wooding, et al. [14], and that of Antonia and Luxton [12]. The data of O'Laughlin was obtained in an air duct 0.11 m by 0.46 m in cross-section and 7.31 m long. Cubes 4.8 mm on a side covered one of the 0.46 m walls of the duct and shear stress was measured directly using a force plate. The closest cube spacing used by O'Laughlin provided a ratio of λ_e/k, in present notation, of 64 and one result, inferred from reference 14, is plotted in Fig. 1. Agreement is not good in this case, perhaps because of the rather small duct size used by O' Laughlin.

Antonia and Luxton studied a boundary layer developing over square bars placed normal to the flow such that $\lambda_e/k = 4$. For large x/k, ($x/k \gtrsim 250$) H became constant and then decreased with increasing x, from which the authors assumed that an equilibrium condition had been reached. The data quoted here is for $x/k = 372$. For $\lambda_e/k = 4$, it is likely that the bars are so close together that mutual sheltering takes place. This is anticipated by Dvorak's results [8] and by the limitation $\lambda_e/k > 5$ placed on equation (2). We expect, therefore that the nondimensional shear stress (U_τ/U_1) would be lower than, but close to, that calculated for $\lambda_e/k = 5$. The data from Antonia and Luxton's report [12], plotted in Fig. 1, confirms this expectation.

The data from the present experiments plotted in Fig. 2 do not all show good agreement with the plotted curves which were calculated using the assumption of equilibrium. As is clearly seen from the figure, the measured values do approach the expected equilibrium, and are quite well given by the appropriate equilibrium curve ($\lambda_e/k = 30$) for the two smallest values of n (i.e., the two largest values of x/k). We therefore conclude that a roughness fetch of approximately 350 k is required to reach equilibrium, at least for the upstream conditions present in this experiment.

Another indication of the present boundary layer's approach to the calculated equilibrium condition is apparent in the values of the defect law integral parameter, $U_1\delta^*/(U_\tau\delta)$, discussed in Section 4. Values of this ratio, deduced from measured shear and n, are given in Table 1 for the present case, and range from 4.27 at the first data point ($x/k \simeq 141$) to 3.92 at the last data point ($x \simeq 493$). The equilibrium value of the ratio, as found from Head's method and the assumption of equilibrium is 3.99 for $\lambda_e/k = 30$ and $n \simeq 0.26$, showing that the present boundary layer becomes very close to the equilibrium condition predicted for it.

From this limited comparison of anticipated and measured results, we conclude that Dvorak's correlation of shear stress with integral boundary layer properties and roughness geometry is useful in predicting rough-wall boundary layer characteristics and that a boundary layer developing over constant wall roughness can approach equilibrium after a rather long ($x/k \gtrsim 350$ in this case) fetch of roughness. The fetch required will certainly vary with the roughness used and the initial conditions imposed, but is not always as large as suggested by Counihan [13] ($x/k \simeq 1{,}000$) on other grounds.

7 Estimating Roughness for Use in Atmospheric Simulations

The roughness required to generate a velocity profile of a given shape with a boundary layer of a given depth can be estimated from the equilibrium results described in Section 4. Great accuracy will not be obtained, for the degree of equilibrium reached in any situation depends on the upstream history of the layer and in particular the fetch used and the trip used (if any). First estimates are possible however, as shown in the following paragraphs.

For example, if a boundary layer is required for simulations of a suburban wind at a scale of 1:400, then a boundary layer of about 0.9 m thick is required with a shape given by $n \doteq 0.28$. If the defect law integral parameter $U_1\delta^*/(U_\tau\delta)$ is about 4 for a boundary layer developing over uniform roughness, as found in the tests described in Section 5, then, from equation (11), δ^*/δ is about 0.22 and U_1/U_τ is therefore about 18. Also, the nominal value of δ^* is about 0.2 m.

Appropriate combinations of roughness, height and density may now be chosen from Fig. 1, since δ^* and U_1/U_τ are known. If 25 mm roughness elements are used, then $\delta^*/k \doteq 8.0$ and for $U_\tau/U_1 = 1/18 = 0.055$, the effective value of λ_e/k is about 14 from Fig. 1. This means that roughness elements with square frontal projections 25 mm square would [from equation (4)] have to be placed on approximately 95 mm centers to provide the correct roughness on the floor. Alternatively, if square elements 40 mm high and 40 mm wide are used, a similar procedure suggests that they should be placed on approximately 175 mm centers.

If the local effective wall shear stress determines the mean characteristics of an equilibrium boundary layer and its important turbulent properties as well (as already assumed in Section 2), then both of the roughness element geometries described will produce identical boundary layers once equilibrium is reached. The important question of which flow would reach equilibrium more quickly requires further investigation and would depend on the initial conditions used in each case.

When exact equilibrium is assumed, as in the present example, predictions can be made directly from Fig. 2. For the required δ and n, combinations of spacing (density) and height can be selected from the figure and give the same results as those calculated in the previous paragraph.

The possibility of using graded roughness, closer spacing or greater height at the start, is an obvious possibility. As an extension of this idea, very large initial roughness elements in the from of spires or wedges have been used to develop the boundary layer (reference [2] or [3]) with much smaller but uniform roughness being used downstream. The likelihood of the boundary layer being close to equilibrium seems somewhat remote in these cases however, unless a very long fetch of roughness is used downstream of the spires. In Counihan's simulation of the urban boundary layer using wedges (reference [3]), the integral parameter $U_1\delta^*/(U_\tau\delta)$ at the point where equilibrium is assumed has a value of over 4.50 whereas present calculations suggest that a value closer to 4.00 would represent equilibrium. More work needs to be done in this area, both to assess the degree of equilibrium present downstream of various spires or graded roughness elements and to assess the importance of equilibrium for the testing being done.

Acknowledgments

Much of the work reported here was started while the first author was on sabbatical leave at the National Research Council of Canada. The cooperation and encouragement of those at the N.R.C. is appreciated, as is the financial support from the N.R.C. through grant A4308 and from the Atmospheric Environmental Service through grant 8103.

References

1 Davenport, A. G., and Isyumov, N., The Application of the Boundary Layer Wind Tunnel to he Prediction of Wind Loading; *Seminar, "Wind Effects on Buildings and Structures,"* Ottawa, Sept., 1967, Proceedings, Vol. I, p. 201.

2 Standen, N. M., "A Spire Array for Generating Thick Turbulent Shear Layers for Natural Wind Simulation in Wind Tunnels," NRC (Canada), NAE LTR-LA-94, May 1972.

3 Counihan, J., "The Structure and the Wind Tunnel Simulation of Rural and Urban Adiabatic Boundary Layers," *Symposium of External Flows*, University of Bristol, July 1972.

4 Townsend, A. A., *The Structure of Turbulent Shear Flow*, Cambridge University Press, 1956.

5 Perry, A. E., Schofield, W. H., and Joubert, P. N., "Rough Wall Turbulent Boundary Layers," *Journal of Fluid Mechanics*, Vol. 37, 1969, p. 383.

6 Rotta, J. C., *Progress in Aero. Sciences*, Vol. 2, Ferri-Pergamon Press, 1962.

7 Mellor, G. L., and Gibson, D. M., "Equilibrium Turbulent Boundary Layers," *Journal of Fluid Mechanics*, Vol. 24, 1966, p. 225.

8 Dvorak, F. A., "Calculation of Turbulent Boundary Layers on Rough Surfaces in Pressure Gradient," *AIAA Journal*, Vol. 7, 1969, p. 1752.

9 Clauser, F. H., "Turbulent Boundary Layers in Adverse Pressure Gradients," *Journal of the Aeronautical Sciences*, Vol. 21, 1954, p. 91.

10 Engineering Sciences Data Unit; Item No. 70015 "Fluid Forces and Moments on Flat Plates," October, 1972, and Item No. 71016, "Fluid Forces, Pressures and Moments on Rectangular Blocks," July, 1973.

11 Gartshore, I. S., "A Relationship Between Roughness Geometry and Velocity Profile Shape for Turbulent Boundary Layers," N.A.E., LTR-LA-140, 1973, National Research Council of Canada.

12 Antonia, R. A., and Luxton, R. E., "The Response of a Turbulent Boundary Layer to a Step Change in Surface Roughness," *Journal of Fluid Mechanics*, Vol. 48, 1971, p. 721.

13 Counihan, J., "Wind Tunnel Determination of the Roughness Length as a Function of the Fetch and the Roughness Density of Three-Dimensional Elements," *Atmospheric Environment*, Vol. 5, 1971, p. 637.

14 Wooding, R. A., Bradley, E. F., and Marshall, J. K., Drag Due to Regular Arrays of Roughness Elements of Varying Geometry," *Boundary Layer Meteorology*, Vol. 5, 1973, p. 285.
